

GEOLOGICAL / GEOTECHNICAL INVESTIGATIONS

ZOJI-LA TUNNEL PROJECT

SRINAGAR, (J & K)

1.0 Introduction:

Ladakh area of Jammu and Kashmir is linked with rest of the country through two routes Leh - Srinagar and Leh – Manali which remain closed in the months of November to March every year due to heavy snow fall. To overcome this isolation of Ladakh region, Boarder Roads Organization has planned two tunnels in the difficult areas of the National Highway 1D.

Proposed Zoji-La tunnel site is located 13km from Sonamarg towards Minamarg (Dras) on the National highway 1D between Baltal and Minamarg. Zoji-La Pass is 9 km from Sonamarg and provides a vital link between Ladakh and kashmir (Fig. 1). It falls at an elevation of approximately 3,528m (11575 ft), and is the second highest pass after Fotu La on the Srinagar –Leh National highway. It remains closed during the months of November to March due to heavy snow fall in the area. Eastern portal of this Zoji-La tunnel is located just 8Km before Minamarg on the left side of the river Dras, whereas the Western portal of the tunnel is located at Baltal on the right side of the river Sindh (Fig. 2).

Geological mapping has been done on 1: 5000 scale during the topographic survey of the area itself. The geological map in this report is being produced on much reduced scale. A number of sections have been developed across the tunnel alignment as well as along the tentative tunnel alignment.

Contributions to these studies have been made by Dr. G.C.S.Gaur and Mr. Ravi Negi of M/S G S GeoEnVirons Pvt. Ltd. And Dr. Mahendra Singh of Civil Engineering Department, IIT Roorkee.

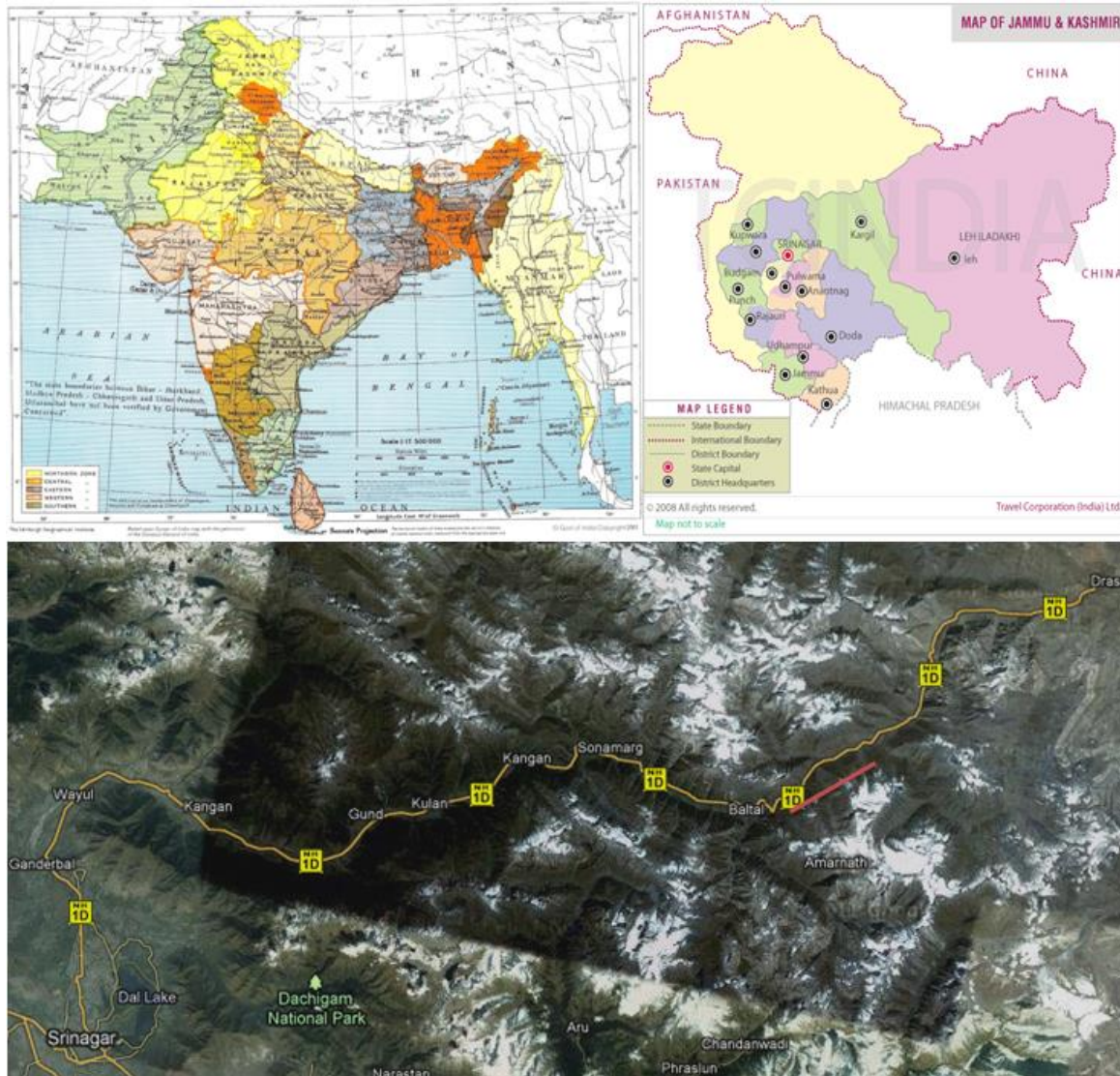


Fig.1 Location map of the project area

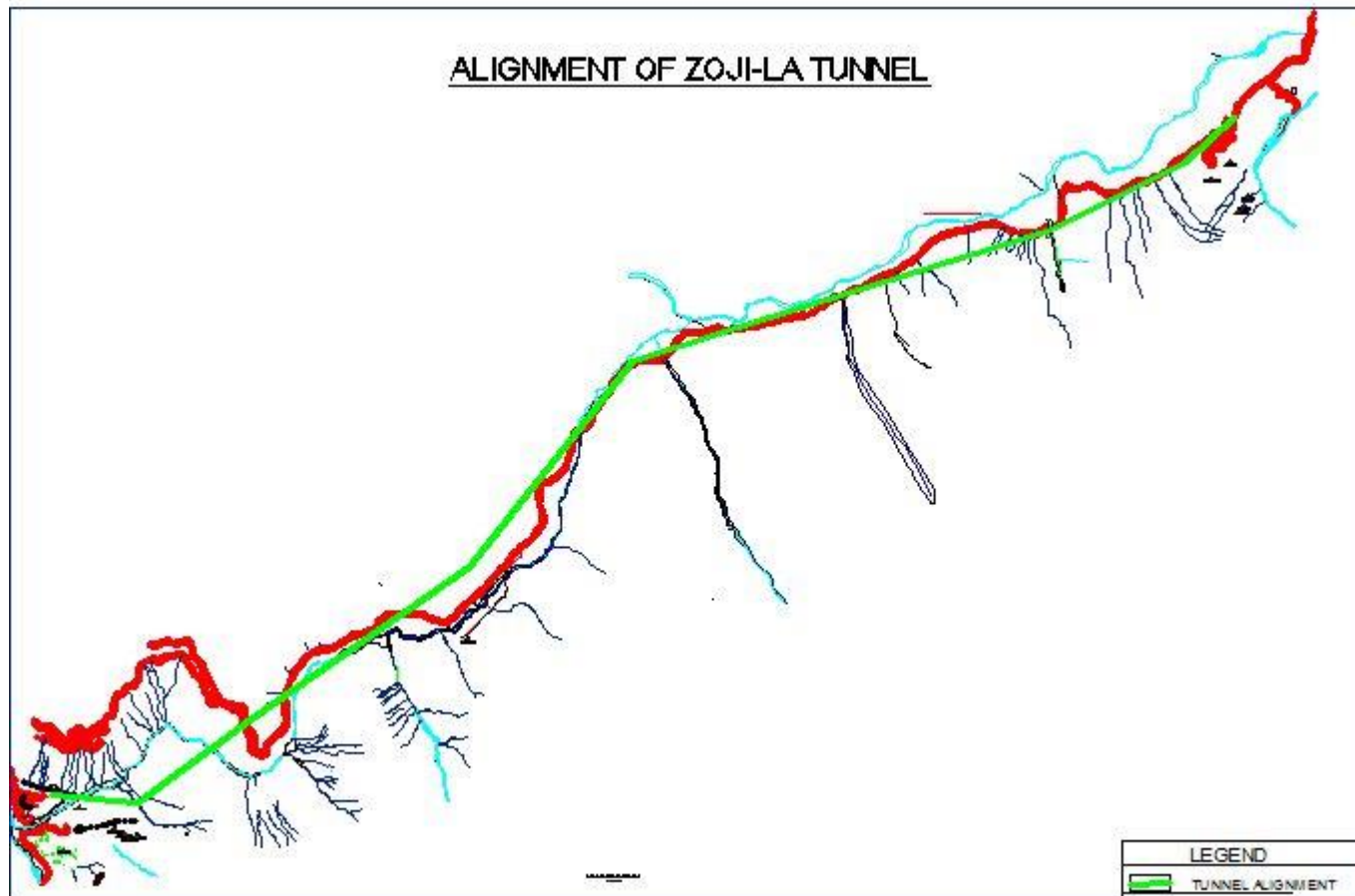


Fig. 2 Proposed Zoji-La Tunnel Alignment

2.0 Geomorphology

The proposed project area exhibits an undulating and rugged topography with highly mountainous, barren terrain. Altitude around the project site varies between 2700 and 4000 m above MSL. Hill faces are made up of vertical cliffs and high escarpments (Fig. 3). Base of the hill faces are covered with slided debris and loose Talus /Scree deposit produced mainly due to frost weathering. Wide valleys of Sonamarg and Baltal areas fall on such slided debris (Fig. 4 and 5). Most of the settlements on lower reaches are also located on slided debris.

The area is marked by well delineated Northeast Southwest trending parallel mountain range.

Project site is located between Sindh and Dras Rivers. Proposed Eastern portal of the project site is located in the Dras valley which starts from the base of Zoji-La Pass whereas Western portal open's in the Sindh valley.



Fig. 3 A view of high cliff and Escarpments.



Fig. 4 A view of Baltal (Sindh River) valley, Sonamarg.



Fig. 5 A view of Dras River valley from Eastern portal of proposed Tunnel.

Area is drained by two mighty turbulent rivers Sindh and Dras, Both rivers are originating from glaciers falling in this areas. High peaks of Amarnath, Thazwas and Sonamarg Glaciers contribute water in the river Sindh and its tributaries, whereas the glaciers of high peaks of Gumri, Machoi and Shytani nallah provide water to river Dras, and its tributaries.

Sindh River one of the largest river of Kashmir, is having gentle gradient and runs through wide valley. In contrast the Dras River in the immediate area forms deep gorge having steep gradient. After Minamarg, Dras river also attains gentle slope within a wide valley.

Geomorphologically the area is in a young stage and erosion is comparatively rapid. The slopes are steep and unstable.

3.0 Regional Geology:

The earliest reference to the geology of Ladakh region is available from the works of Thompson (1852), Stoliczka (1866), Drew (1875), and Lydekker (1880-83). The latter studied the western part of the Ladakh along Sonamarg - Zozi la - Dras belt and followed the classification based on Palaeo-Mesozoic succession of Kashmir (Middlemiss, 1910).

The comprehensive studies including mapping were undertaken by Wadia (1937), in Gilgit and Astor region. In continuation, the work on this belt was carried out by Kohli, Sahni and Bhatnagar (1958).

The Tethyan rocks of Kashmir which override the Indus belt consist chiefly of Triassic-Jurassic sediments, though in the basement high zone of the Nun-Kun axis which extends along the Suru Valley, older rocks override the belt.

Regional geological / lithostratigraphical map of the area is given in the Fig.6 and the Lithostratigraphy of the region is described in the table 01.

Table 01 Lithostratigraphic Succession of the area around Z-Morh.

Facies	Formation	Members
Indus Flych Sediments	Kargil Formation	
	~~ Kargil Thrust or Unconformity ~~	
Indus facies	Dras Formation	Maman Phyllite Serpentine- Chromitite- Dunite Radiolarian chert, Limestone and mélange Lava and agglomerates Changthang slate

	~~~~~ Dras Thrust ~~~~~	
Tethyan facies	Matayin Limestone Zozi la Formation Panjal trap Agglomerate slate Tertiary Granite (Intrusive in Indus facies)	
	~~Kargil Thrust or Unconformity ~~	
Granite Group	Ladakh Granite (Northern basement)	

3.1 Agglomerate slate:

Fine grained gray to black colored sedimentary rock formation is known as Agglomerate slate. Formation is exposed in the core of the Zozi- La anticline between Gumri nallah and Machoi nallah. This formation consists of dark colored slates and grey colored Phyllites with alternating bands of Pyrite greywacke.

This assemblage lithologically resembles with the Agglomeratic slates from rest of Kashmir. The Agglomerate slates are the oldest exposed unit in the Zozi –La anticline,

This formation is underlain by the Panjal trap.

3.2 Panjal trap:

The Agglomeratic slate is overlain by a band of green partly schistose basic lava, which is considerably metamorphosed giving resemblance of green schist. The volcanic textures and structures such as the pillows are often faithfully preserved at a number of places, especially near Minamarg.

A small patch of Panjal trap is also exposed near Zoji- La within another small anticline and is visible on the cliff to the east of the Pass.

3.3 Zoji- La Formation:

A large severely folded belt comprising of grey and brown Phyllites with bands of limestone's and pyritic shale, is found exposed immediately overlying the Panjal trap in the area and is in turn overlain by the thick massive Matayain Limestone.

On the basis of Fragments of fossil Ptychites found at Thajwas, it has been referred as Muschelkalk by many workers. This formation has been given the name "Serzing phyllite" by Raiverman and Mishra (op.cit) in the eastern part, but they have made no reference to the western outcrop in Zoji-la and Thajwas.

In the Zoji-la Section, the rock comprises brown, limonitic, sandy and schistose slate and phyllite at the base, followed by thinly bedded grey slate and calcilutite with occasional bands of calcarenite.

3.4 Matayin Limestone:

Throughout the southern part of the area a thick zone of limestone, partly dolomite, is found exposed from Sonamarg to southeast of Dras and from Gyal through south of Mulbekh. In the Sonamarg- Baltal section this limestone is exposed in a syncline flanked by the Zoji-La formation of Thajwas and Zoji-La on either side. In Matayin, it overlies conformably the Zoji-La formation and in the east it has been partly cut off by Dras thrust.

In the Zoji-La section, the upper part of Zoji-La formation consist of black shale which passes gradually upwards in to thin bedded platy limestone having frequent marly bands and topped by a considerable thickness of massive dolomite.

3.5 Dras Formation

Dras formation is over 3,000m thick and consists of a complex of sedimentary and igneous suite of rocks. The basal unit of the formation exposed in the east near Changthang and persisting through Shergol to Namikala, consist mostly of dark grey slates, slaty shale and occasional limestone, with which bands of greywacke and purple radiolarian chert are interbedded.

The middle unit consists of enormous thickness of basic lava, agglomerate, tuff, ash beds and numerous bands of lensoid jasperite, chert, calcilutite and shale.

The upper part of the Dras formation comprises a thick suite of severely controlled calcareous phyllite with interbedded chert and greywacke. It lies in immediate contact with the Dras Thrust.

3.6 Kargil Formation

In the Kargil area the formation rests unconformably on the Ladakh Granite and has a gentle southerly dip, the contact being marked by a zone of conglomerate containing boulders of granite and rocks of Dras Formation. This is succeeded by a thick sequence of sandstone and shale containing fresh water mollusks. The southern limit of Kargil belt is bound by a thrust, the Kargil Thrust, along which the Dras Formation comes in juxtaposition with these rocks. The upper part is thus truncated by a thrust and accordingly the complete thickness of the formation is not exposed.

The belt continues eastwards within the same tectonic setting as far as Hagins-Shakardeo. A noteworthy feature is that there is a continuous lateral and vertical variation of facies, with the addition of new lithological elements towards the base. The conglomerate-sandstone sequence in Hagins is not the basal unit but lies towards the middle whereas the base consists of a sequence of dark-grey shale-greywacke rhythmites. This zone becomes very thick to the east in Khalsi and beyond, where almost a complete sequence of greywacke, shale and limestone rhythm is exposed. This facies of rocks has usually been referred to as "Indus Flysch" while the Kargil sequence as "Ladakh Molasse".

It is interesting to note that the “flysch” facies in the eastern part is a marine one as is evidenced from the presence of marine foraminifera, suggesting an early to the late Cretaceous age, (Pande *et. al.*, 1969), whereas the “molasse” of Kargil indicates a fresh water facies as indicated by its fauna and it is essentially Tertiary in age. This is a case of lateral and vertical variation of facies wherein the Cretaceous “flysch” sequence passes outwards to southwest and upwards into Tertiary “Molasse” sequence. Equivalents of Kargil Formation are also exposed to south of the main belt resting directly on the folded Dras Formation. These rocks occur as outliers, like the outcrops of Cheskor and Batambas, or are caught up within the imbricate structures of the Dras Formation towards the southern part of the Dras belt.

4.0 Geology of the area

Geological mapping has been carried out on 1:5000 scales, but is being produced here on a reduced scale (Fig. 7). Detailed structural data has been collected and plotted on the same scale (Fig. 8). A series of geological sections have been developed based on the surface data for geological interpretation (Fig. 9 to 24).

Lithostratigraphy in the area can be described as follows:

Recent	River born material
	Debris and Talus material
	Permafrost Soil
	Palaeoglacial deposits
	~~~~~
<b>Permo- Carboniferous</b>	Zoji- La Formation
	Panjal Trap
	Agglomerate Slates



#### **4.1 River Born material:**

River Born Material is found deposited along the river bed. It consists of loose large boulders, pebbles, grit, sand and silt. This material is continuously modified during the floods.

#### **4.2 Debris and Talus Material:**

Thick amount of Debris materials are found all along the base of the hill faces and along the wide valleys. Debris materials are product of physical (frost) weathering at the top of the ridge from where it flows downwards and consists of coarse angular fragments. These rock fragments are often found embedded in the loose grit, sand silt and clay. The slided debris consists of angular fragments of varying sizes embedded in the fine matrix of grit, sand, silt and clay.

**Page insert**

Fig 9 – L Section along Tunnel Alignment

Fig 10 X- Section along E Portal

Fig 11 X Section along .....

Fig 12

Fig 13

Fig 14

Fig 15

Fig 16

Fig 17

Fig 18

Fig 19

Fig 20

Fig 21

Fig 22

Fig 23

Fig 24 X Section along Western portal

### **4.3 Permafrost Soil**

Fine grained brown-black color permafrost soil is found in the area of project site. These soils are generally found where the freezing conditions are found for major part of the year.

### **4.4 Palaeoglacial deposit**

In the area receding glaciers have left sediments along the flank of valleys consisting of angular boulders and pebbles embedded in huge fine grained angular sediments. At present these deposits have already been modified due to fluvial process and have been loaded with talus/scree material.

### **4.5 Zoji-La Formation**

Large severely folded units consisting of dark grey graphitic phyllites are found in the eastern part of the project. These phyllites are finely foliated in which fine platy minerals impart shining texture to the rocks. Along the foliation planes extremely fine grained lenticular silica veins are observed. At places within these phyllites fine pyrite cubes are noted in abundance (Fig. 25).

Slaty cleavage is also noted at certain places within these phyllites (Fig. 26). In the area, these phyllites have near vertical dip of foliation. Rocks are also jointed, but these joints do not persist for long (Fig. 27).

In the core of Zoji-La anticline brown limonitic, sandy and schistose slates and phyllite are found. These slates grade upward into dark grey slates and calcilutite with occasional fine bands of calcarenite.



Fig .25 A Close view of Zoji-La Slates, in which fine purite cubes are noted in abundance



Fig. 26 A View of Zoji-La Formation near Captain morh, where dip of foliation is nearly vertical





Fig. 27 A View of Zoji-La formation having steep foliation and three set of joints.

#### 4.6 Panjal Trap

Dark green colored basic rocks belonging to Panjal Trap are found in the proposed project site area underlain by Zoji-La formation. Often these meta-basics due to leaching give brown color to the rocks. Panjal Traps are found on the Eastern and western margin of the area, as well as in the central part also due to Anticlinal folding. Along eastern portal Trap have wide exposure on the ground compared to exposure in the central and western parts. Hard, compact, meta-basic rocks are massive, slaty and often schistose. 1-20m thick different types of trap are being observed in the project area.

Fine grained trap having glossy texture is observed in the central part. These rocks exhibit homogenous texture and color and are characterized by curved fractures (Fig. 28). Generally these are massive traps. Slaty schistose traps are thinly foliated slightly sheared and highly jointed.



Fig. 28 A View of Curve fracture after Shytani nallah.



Fig. 29 A close View of Fine grained Porphyroblastic Panjal Trap rock





Fig. 30 A Close View of Vesicular structure in fine grained basic rocks.



Fig. 31 A View of Panjal Trap Formation



Fig. 32 A View of Vesicular basic rocks, Vesicles filled by Secondary minerals.

Panjali Trap rocks are fine to medium grained and rich in basic minerals assemblage like Amphiboles, Hornblende, Plagioclase and Olivine (Fig 29). Amphiboles and Plagioclase mineral assemblage dominates throughout the whole lava flow sequence. Serpentine veins are also noted in these rocks. These rocks are dominantly basaltic-andesitic and show a compositional and environmental affinity with accreting plate margin lava. Vesicular structures are often found in the rock formation (Fig 30).

Rocks are mostly fresh, but often shallow weathering is noted at certain places. Leaching of iron minerals is also profound in the area, which imparts brown color to the rock on the surface. The Panjali Traps are greenish to brownish color rocks with some dark grey variations (Fig 31). They are very hard, compact; massive, and generally fine-grained. Compact mass of fine grained material often shows amygdaloidal structure. Chlorite, Quartz, Calcite and Epidote filling are found in the cavities (Fig. 32). In some schistose basic rocks chlorite is found developed along the foliation plane (Fig. 33). Vesicular structure is also found in these traps. The vesicles, range in size from small speck to more than 5 cm (longest-axis). Most of the vesicles are elongated in shape. Whereas rounded vesicles are also noted in the area. Quartz veins are



commonly found traversing these rocks along bedding planes, joints and fractures (Fig.34).



Fig. 33 A View of schistose basic rock in which Chloritic flakes are found oriented along foliation planes



Fig. 34 A View of schistose basic rock in which Quartz Veins are found along foliation planes

The Panjal Traps are made up of semi crystalline aggregate of Plagioclase, Amphiboles and Pyroxene with a mesostasis in which microlites of these minerals and their alteration products are found embedded in the devitrified glass in the groundmass. Opaque minerals, varying in size from fine microscopic dust to small microphenocrysts, are common throughout the whole sequence of lava beds. Coarse grained hornblende crystals provide porphyritic texture to the rocks.

In the microscopic observations Plagioclase minerals occur in three sizes—megaphenocrysts, microphenocrysts, and minute microlites. Megaphenocrysts, sometimes altered to kaolin, are noted at some locations whereas; the microphenocryst and microlites form a common feature of this lava sequence. The megaphenocrysts, in general, and some microphenocrysts are fractured in which these fractures are often healed up with green chlorite and epidote.

The composition of the plagioclase is variable and has a close correlation with the size of this mineral. The magaphenocrysts, are highly calcic; their compositional range is between Bytownite and labrodorite ( $An_{82}-An_{56}$ ). The composition changes from calcic to sodic plagioclase with the decrease in size of the phenocrysts. Zoning towards decreasing An-content is observed along the peripheral portion of some crystals.

Hornblende, pyroxene, olivine are other dominating minerals in the assemblage. Pyrite cubes are found in the ground mass as minor mineral.

#### **4.7 Agglomerate Slate:**

This formation is consists of greywacke and slates with angular fragments of quartz-porphyry, granite, slate, etc. These clasts are dispersed irregularly in the rock mass (Fig. 35).





Fig. 35 A View of Agglomerate slate Formation



Fig. 36 A close View of Fine grained Agglomerate slate.

Agglomerate slates are found in the central reach of the area in an anticlinal core. Greywakes are fine to coarse grained and are having fine layers of platy minerals along the foliation planes (Fig 36).

In the microscopic observation this rock formation showing fine grained acidic volcanic rocks fragments and the occurrence of devitrified glass in the large amount in the matrix that indicates that the debris constituting the Agglomeratic slates is of pyroclastic origin.

The most important among these is the presence of fractured quartz grains which are held together exactly in their original position, the cracks being often filled with dirty brown glass of the same character as that constitutes the matrix.

Another feature of microscopic studies is the replacement of detrital quartz grains by sericite. It is obvious that much chemical readjustment has taken place between the clastic grains and enclosing matrix after the deposition of pyroclastic debris.

## 5.0 STUCTURE OF THE AREA

Rocks are found all over the project area and it was easy to observe the structural data. Most of the area was not accessible, still fair amount of data has been collected from all over the area.

### 5.1 Foliation:

Foliation planes are marked by sheet differentiations in the rocks. Orientation of flaky minerals and their colour also define the foliation planes. Rocks are having Steep to moderate dip of the foliation in the entire area. Rocks of Zoji-la Formation and Agglomerate Slates are thinly foliation whereas rocks of Panjal Trap are thickly to thinly foliated, foliation planes are well marked in all the formations (Fig 37 to 40).

The foliation varies as follows:

Location	Strike	Dip	Direction
At Proposed Eastern Portal	N 71° - N 251°	58°	N 161°
Along the ridge near E. portal location	N 61° - N 241°	57°	N 151°
Between Eastern Portal & Machoi Nallah hill side	N 64° – N 244°	57°	N 164°
Near the bend of Machoi nallah road side	N 145° – N 325°	67°	N 235°
Right side of Machoi nallah	N 80° – N 260°	78°	N 170°
Left side of Machoi nallah	N 75° – N 255°	81°	N 165°
Between Shytani nallah and Machoi nallah	N 145° – N 325°	62°	N 235°
Near the Shytani nallah	N 99° – N 279°	73°	N 189°
Between Gumri & Shytani nallah	N 88° – N 268°	73°	N 178°
Right side of Gumri Nallah	N 12° – N 192°	59°	N 282°

Near the last end of right side of Gumri Nallah	N 98 ⁰ – N 278 ⁰	76 ⁰	N 188 ⁰
Left side of Gumri Nallah	N 35 ⁰ – N 215 ⁰	64 ⁰	N 305 ⁰
Near the Gumri nallah	N 15 ⁰ – N 195 ⁰	55 ⁰	N 285 ⁰
Near Zoji-La Pass	N 14 ⁰ – N 194 ⁰	54 ⁰	N 284 ⁰
Zoji-La Pass area	N 35 ⁰ – N 215 ⁰	62 ⁰	N 305 ⁰
Right side of the Fall	N 65 ⁰ – N 245 ⁰	76 ⁰	N 335 ⁰
Left side of the Fall	N 61 ⁰ – N 241 ⁰	82 ⁰	N 331 ⁰
Near the Captain morh	N 65 ⁰ – N 245 ⁰	76 ⁰	N 335 ⁰
Captain morh area on the road	N 85 ⁰ – N 265 ⁰	76 ⁰	N 355 ⁰
Western portal location	N 72 ⁰ – N 252 ⁰	76 ⁰	N 342 ⁰
Near the Area of proposed Western portal	N 75 ⁰ – N 255 ⁰	78 ⁰	N 345 ⁰

## 5.2 Joints:

Rocks are highly jointed and fractured. Three sets of joints are most predominant in the area followed by minor joints. All the major joints persist for quite long distance. Often along these joints weathering is noted for some depth. Orientation diagram of these joints have been plotted on stereo net and being given in Fig (41 to 46). Joint sets in the different rock types show different orientation and characters (Fig 37 to 40) along certain joints shearing is also noted.

The prominent major joint sets and there characteristics are as follows:

**Prominent Joint sets near the Eastern portal, Zoji-La**

Sets No.	Strike	Dip	Directions	Remarks	Description of Discontinuities
1	N160 ⁰ - N340 ⁰	30 ⁰	N 250 ⁰	Open joint set with the gap of 1-2 cm, filled with clay & weathered materials. Persist for 10 to 12m. 2 to 3m apart.	Rough (Undulating)
2	N66 ⁰ - N 246 ⁰	55 ⁰	N 156 ⁰	Open joint with the gap of 1-2cm filled with clay and weathered materials Persist for 8 to 10m. 1 to 2m apart.	Rough (Steep)
3	N 45 ⁰ - N 225 ⁰	23 ⁰	N 315 ⁰	Open joint with the gap of 1 cm filled with clay and weathered gravel soil material. Persist for 10 to 12m. 3 to 4 m apart.	Rough (Undulating)

**Prominent Joint sets between Eastern Portal and Machoi nallah area, Zoji-La**

Sets No.	Strike	Dip	Directions	Remarks	Description of Discontinuities
1	N135 ⁰ -N315 ⁰	15 ⁰	N 225 ⁰	Open joint with the gap of 1 cm filled with clay and weathered material. Persist for 15-18m. 3 to 4 m apart.	Rough (Planar)
2	N175 ⁰ -N 355 ⁰	43 ⁰	N 265 ⁰	Open joint with the gap of 1 cm filled with clay and weathered material. Persist for 12-15m. 2 to 3 m apart.	Smooth (Steeped)
3	N155 ⁰ -N 335 ⁰	53 ⁰	N 65 ⁰	Open joint with the gap of 1-2 cm	Rough



				filled with clay and weathered material. Persist for 18 to 20m. 2 to 3 m apart	(Undulating)
--	--	--	--	--------------------------------------------------------------------------------	--------------

### Prominent Joints sets on the right side of Machoi nallah

Sets No.	Strike	Dip	Directions	Remarks	Description of Discontinuities
1	N 63 ⁰ - N 243 ⁰	56 ⁰	N 153 ⁰	Open joint with the gap of 2-3 cm filled with clay and weathered materials. Persist for 12-15m.	Rough ( Steeped)
2	N145 ⁰ - N325 ⁰	15 ⁰	N 235 ⁰	Open joint with the gap of 1-2cm filled with clay and weathered materials. Persist for 18-20m. 3 to 4m apart.	Rough (Planar)
3	N155 ⁰ - N335 ⁰	53 ⁰	N 245 ⁰	Open joint with the gap of 1 cm filled with clay and weathered material. Persist for 20-22m. 3 to 5 m apart.	Rough ( Steeped)

### Prominent Joints sets on the left side of Machoi nallah

Sets No.	Strike	Dip	Directions	Remarks	Description of Discontinuities
1	N145 ⁰ -N 325 ⁰	56 ⁰	N 55 ⁰	Open joint with the gap of 1-3 cm filled with clay and weathered materials. Persist for 20-22m. 3 to 5 m apart.	Rough (Steeped)
2	N130 ⁰ -N 310 ⁰	69 ⁰	N 40 ⁰	Open joint with the gap of 1-2cm	Rough (Steeped)

				filled with clay and weathered materials. Persist for 18-20m. 3 to 4 m apart.	
3	N 55 ⁰ - N235 ⁰	53 ⁰	N 145 ⁰	Open joint with the gap of 1 cm filled with clay and weathered material. Persist for 20-22m. 3 to 5 m apart.	Rough (Steeped)
4	N160 ⁰ -N 340 ⁰	47 ⁰	N 69 ⁰	Open joint with the gap of 0.5-1 cm filled with clay and weathered material. Persist for 20-22m. 1 to 3 m apart.	Rough (Steeped)

#### Prominent joints between Shytani nallah and Machoi nallah

Sets No.	Strike	Dip	Directions	Remarks	Description of Discontinuities
1	N 15 ⁰ - N 195 ⁰	32 ⁰	N 105 ⁰	Open joint with the gap of 1 cm filled with clay and weathered material. Persist for 15-18m. 3 to 4 m apart.	Rough (Undulating)
2	N136 ⁰ -N 316 ⁰	57 ⁰	N 46 ⁰	Open joint with the gap of 1 cm filled with clay and weathered material. Persist for 12-15m. 2 to 3 m apart.	Rough (Undulating)
3	N150 ⁰ -N 330 ⁰	36 ⁰	N 240 ⁰	Open joint with the gap of 1-2 cm filled with clay and weathered material. Persist for 18 to 20m. 2 to 3 m apart.	Slickenside (Undulating)
4	N110 ⁰ -N 290 ⁰	52 ⁰	N 200 ⁰	Open joint with the gap of 1 cm filled with clay and weathered	Smooth (planar)

				material. Persist for 15 to 18m. 1 to 3 m apart.	
5	N115 ⁰ -N 295 ⁰	70 ⁰	N 25 ⁰	Open joint with the gap of 1 cm filled with clay and weathered material. Persist for 15 to 18m. 1 to 3 m apart.	Rough (Steeped)

### Prominent Joints sets on the right side of Gumri nallah

Sets No.	Strike	Dip	Directions	Remarks	Description of Discontinuities
1	N135 ⁰ -N315 ⁰	21 ⁰	N 45 ⁰	Open joint with the gap of 0.5-2 cm filled with clay and weathered material. Persist for 15 to 20m. 2 to 3 m apart.	Rough (Undulating)
2	N147 ⁰ -N 327 ⁰	25 ⁰	N 57 ⁰	Open joint with the gap of 1-2 cm filled with clay and weathered material. Persist for 25 to 30m. 3 to 4 m apart.	Rough (Undulating)
3	N 35 ⁰ - N 215 ⁰	38 ⁰	N 125 ⁰	Open joint with the gap of 1-2 cm filled with clay and siliceous material. Persist for 20 to 22m. 3 to 5 m apart.	Rough (Planar)
4	N 85 ⁰ - N 265 ⁰	31 ⁰	N 175 ⁰	Open joint with the gap of 1-2 cm filled with clay and siliceous material. Persist for 15 to 20m. 2 to 4 m apart.	Rough (Planar)
5	N 40 ⁰ - N 220 ⁰	67 ⁰	N 310 ⁰	Open joint with the gap of 1-2 cm filled with clay and siliceous material. Persist for 15 to 18m.	Rough (Steeped)

**Prominent Joints sets on the left side of Gumri nallah**

Sets No.	Strike	Dip	Directions	Remarks	Description of Discontinuities
1	N120 ⁰ -N 300 ⁰	27 ⁰	N 210 ⁰	Open joint with the gap of 0.5-2 cm filled with clay and weathered material. Persist for 15 to 20m. 2 to 3 m apart.	Rough (Planar)
2	N160 ⁰ -N 340 ⁰	25 ⁰	N 70 ⁰	Open joint with the gap of 1-2 cm filled with clay and weathered material. Persist for 25 to 30m. 3 to 4 m apart.	Rough (Planar)
3	N 75 ⁰ - N 255 ⁰	38 ⁰	N 165 ⁰	Open joint with the gap of 1-2 cm filled with clay and siliceous material. Persist for 20 to 22m. 3 to 5 m apart.	Rough (Undulating)

**Prominent Joints sets near Gumri area**

Sets No.	Strike	Dip	Directions	Remarks	Description of Discontinuities
1	N 49 ⁰ - N 229 ⁰	21 ⁰	N 139 ⁰	Open joint with the gap of 0.5-1 cm filled with clay. Persist for 12 to 15m. 0.50 to 1 m apart.	Rough (Undulating)
2	N 45 ⁰ - N 225 ⁰	15 ⁰	N 135 ⁰	Open joint with the gap of 1-2 cm filled with clay and weathered material. Persist for 10 to 12m. 2 to 3 m apart.	Rough (Planar)
3	N152 ⁰ -N 332 ⁰	37 ⁰	N 242 ⁰	Open joint with the gap of 1-1.5 cm filled with clay and weathered	Rough (Undulating)

				material. Persist for 10 to 12m. 2 to 3 m apart.	
4	N154 ⁰ - N334 ⁰	76 ⁰	N 64 ⁰	Open joint with the gap of 1-2 cm filled with clay. Persist for 15-18m. 1 to 4 m apart.	Rough (Steeped)

### Prominent Joint sets near Zoji-La Pass, road section

Sets No.	Strike	Dip	Directions	Remarks	Description of Discontinuities
1	N156 ⁰ -N336 ⁰	15 ⁰	N 66 ⁰	Open joint with the gap of 1-2 cm filled with clay and weathered material. Persist for 10 to 12m. 2 to 3 m apart.	Smooth (Planar)
2	N170 ⁰ -N 350 ⁰	55 ⁰	N 80 ⁰	Open joint with the gap of 1-1.5 cm filled with clay and weathered material. Persist for 10 to 12m. 2 to 3 m apart.	Smooth (Steeped)
3	N134 ⁰ -N 314 ⁰	83 ⁰	N 44 ⁰	Open joint with the gap of 1-2 cm filled with clay. Persist for 15-18m. 1 to 4 m apart.	Rough (Steeped)
4	N115 ⁰ -N 295 ⁰	55 ⁰	N 205 ⁰	Open joint with the gap of 1-2 cm filled with clay. Persist for 15-18m. 1 to 4 m apart.	Rough (Steeped)

**Prominent Joint sets near Zoji-La Pass**

Sets No.	Strike	Dip	Directions	Remarks	Description of Discontinuities
1	N173 ⁰ - N353 ⁰	22 ⁰	N 83 ⁰	Open joint with the gap of 1-2 cm filled with clay and weathered material. Persist for 10 to 12m. 2 to 3 m apart.	Rough (Undulating)
2	N 05 ⁰ - N 185 ⁰	12 ⁰	N 95 ⁰	Open joint with the gap of 1-1.5 cm filled with clay and weathered material. Persist for 10 to 12m. 2 to 3 m apart.	Rough (Planar)
3	N161 ⁰ -N 341 ⁰	33 ⁰	N 71 ⁰	Open joint with the gap of 1-2 cm filled with clay. Persist for 15-18m. 1 to 4 m apart.	Rough (Undulating)
4	N145 ⁰ - N325 ⁰	28 ⁰	N 55 ⁰	Open joint with the gap of 1-2 cm filled with clay. Persist for 15-18m. 1 to 4 m apart.	Rough (Undulating)

**Prominent Joint sets on the right side of fall, Zoji-La Pass**

Sets No.	Strike	Dip	Directions	Remarks	Description of Discontinuities
1	N175 ⁰ -N355 ⁰	31 ⁰	N 265 ⁰	Open joint with the gap of 0.5-1cm filled with clay and weathered material. Persist for 50 to 55m. 4 to 6m apart.	Rough (Undulating)
2	N15 ⁰ -N195 ⁰	37 ⁰	N 35 ⁰	Closed set of joint Persist for 30-35m. 4 to 5m apart.	Rough (Undulating)
3	N82 ⁰ -N262 ⁰	51 ⁰	N 352 ⁰	Open joint with the gap of 1 cm	Rough (Planar)

				filled with clay and weathered material, Persist for 20-22m. 3 to 4m apart.	
4	N155°-N335°	72°	N 65°	Open joint with the gap of 1 cm filled with clay and weathered material. Persist for 20-22m. 4 to 5m apart.	Smooth (Planar)
5	N144°-N 324°	13°	N 55°	Open joint with the gap of 1 cm filled with clay and weathered material. Persist for 30-32m. 3 to 4m apart.	Rough (Undulating)

**Prominent Joint sets on the Left side of fall, Zoji-La Pass on the road section**

Sets No.	Strike	Dip	Directions	Remarks	Description of Discontinuities
1	N155°-N 335°	21°	N 65°	Open joint with the gap of 0.5-1cm filled with clay and weathered material. Persist for 50 to 55m. 4 to 6m apart.	Rough (Undulating)
2	N 6°- N 186°	7°	N 96°	Open joint with the gap of 1 cm filled with clay and weathered material, Persist for 18-22m. 3 to 4m apart.	Rough (Undulating)
3	N 75°- N 255°	37°	N 165°	Open joint with the gap of 1 cm filled with clay and weathered material, Persist for 20-22m. 3 to 4m apart.	Rough (Undulating)
4	N147°-N 327°	31°	N 57°	Open joint with the gap of 1 cm filled with clay and weathered material. Persist for 20-22m.	Rough (Undulating)



**Prominent Joint sets near the Captain Morh area**

Sets No.	Strike	Dip	Directions	Remarks	Description of Discontinuities
1	N 45 ⁰ - N 225 ⁰	25 ⁰	N 135 ⁰	Open joint with the gap of 0.5-1cm filled with clay and weathered material. Persist for 50 to 55m. 4 to 6m apart.	Smooth (Planar)
2	N105 ⁰ -N 285 ⁰	78 ⁰	N 15 ⁰	Open joint with the gap of 1-2 cm filled with clay and weathered material, Persist for 15-20m. 3 to 4m apart.	Rough (Planar)
3	N 155 ⁰ - N 335 ⁰	16 ⁰	N 65 ⁰	Open joint with the gap of 1 cm filled with clay and weathered material, Persist for 18-22m. 3 to 4m apart.	Rough (Undulating)
4	N 35 ⁰ - N 215 ⁰	7 ⁰	N 125 ⁰	Open joint with the gap of 1 cm filled with clay and graveled material. Persist for 20-22m. 4 to 5m apart.	Smooth (Planar)

**Prominent Joint sets near the Western portal**

Sets No.	Strike	Dip	Directions	Remarks	Description of Discontinuities
	N03 ⁰ -N 183 ⁰	36 ⁰	N 93 ⁰	Open joint with the gap of 0.5-5cm filled with clay and gravel soil material. Persist for 10 to 12m. 2 to 4m apart.	Rough (Undulating)
2	N 98 ⁰ - N 278 ⁰	56 ⁰	N 8 ⁰	Open joint with the gap of 1-7cm	Rough (Planar)

				filled with clay and siliceous veins. Persist for 15 to 18m. 2 to 5m apart.	
3	N 51°- N 231°	63°	N 141°	Open joint with the gap of 1.5 -2 cm filled with clay and weathered material, Persist for 20-22m. 3 to 4m apart.	Rough (Undulating)
4	N 25°- N 205°	67°	N 295°	Open joint with the gap of 0.5 - 2 cm filled with clay and weathered material. Persist for 12-15m.	Rough (Undulating)



Fig. 37. A View of joint set in Panjal Trap near Gumri



Fig.38 A View of joint sets in Basic rock



Fig. 39 A View of joint set in Steep dip foliated Agglomerate formation at Gumri nallah





Fig. 40 A View of Three set of joints in Steep dip foliated Zoji-La formation near Zoji-La Pass

**Page Insert**

Fig 41 Stereographic net

Fig 42

Fig 43

Fig 44

Fig 45

Fig 46 Stereographic net

### 5.3 Fracture & Shear Zone:

Curved fractures are noted at many places mainly in the Agglomerates slates and Panjal Traps (Fig. 28). Most of them are observed along the road sections near the Sytani nalla and Machoi nalla (Fig. 47). Shearing is not observed along these fractures.

At places shear zones as thick as 10 to 15cm are noted. Most of these shear zones are along certain joint planes, where crusted /sheared material is observed as gauge. At places displacements are also noted along these shear planes (Fig 48).

Main orientations of these fractures are as follows:

Serial no.	Dip of Curvature	Orientation
Panjal Trap	43 ⁰	N 232 ⁰
Agglomerate slates	23 ⁰	N 172 ⁰



Fig.47 A View of Curved fracture near Shytnani nallah



Fig. 48 A View of Shear zone area near West portal

#### 5.4 Miner fault:

At certain places minor displacement of foliation planes and joints is observed along a fault, joint plane. The orientation of such planes is  $63^{\circ}$  due N  $143^{\circ}$ .

Displacement is shown in the Fig 49.





Fig. 49 A View of Miner Displacement along joint in Agglomerate slates near Shytani nallah

## 5.5 Folding:

Folding is also observed in the area of such folding is more evident in the Panjal Trap (Fig .50).

Plunge of the fold is  $18^{\circ}$  due N  $271^{\circ}$ .



Fig. 50 A View of Anticlinal Fold in Panjal Trap

## 5.6 Ground Water Conditions

As such the rocks are basically nonporous, impermeable but the joints, fracture and shear provide considerable permeability to the formations. The ground water reservoir conditions are not observed within these rocks. Weathered surface and Scree / Talus deposits are acting as good source for ground water storage.

Area remains capped by snow at higher elevations and water keeps on flowing through channels. Water also percolates through fractures, joints and shear planes (Fig. 51). As such ground water conditions are not favorable in the rocky area.



Fig. 51 A View of Ground water percolation through Joint plain





Fig. 52 A View of proposed Eastern Portal of Zoji-La Tunnel



Fig. 53 A View of Proposed Western Portal of Zoji-La Tunnel



Fig.54 Alignment View of Zoji-La Tunnel near Captain Morh area



Fig. 55 Alignment View of Zoji-La Tunnel near Gumri Camp area



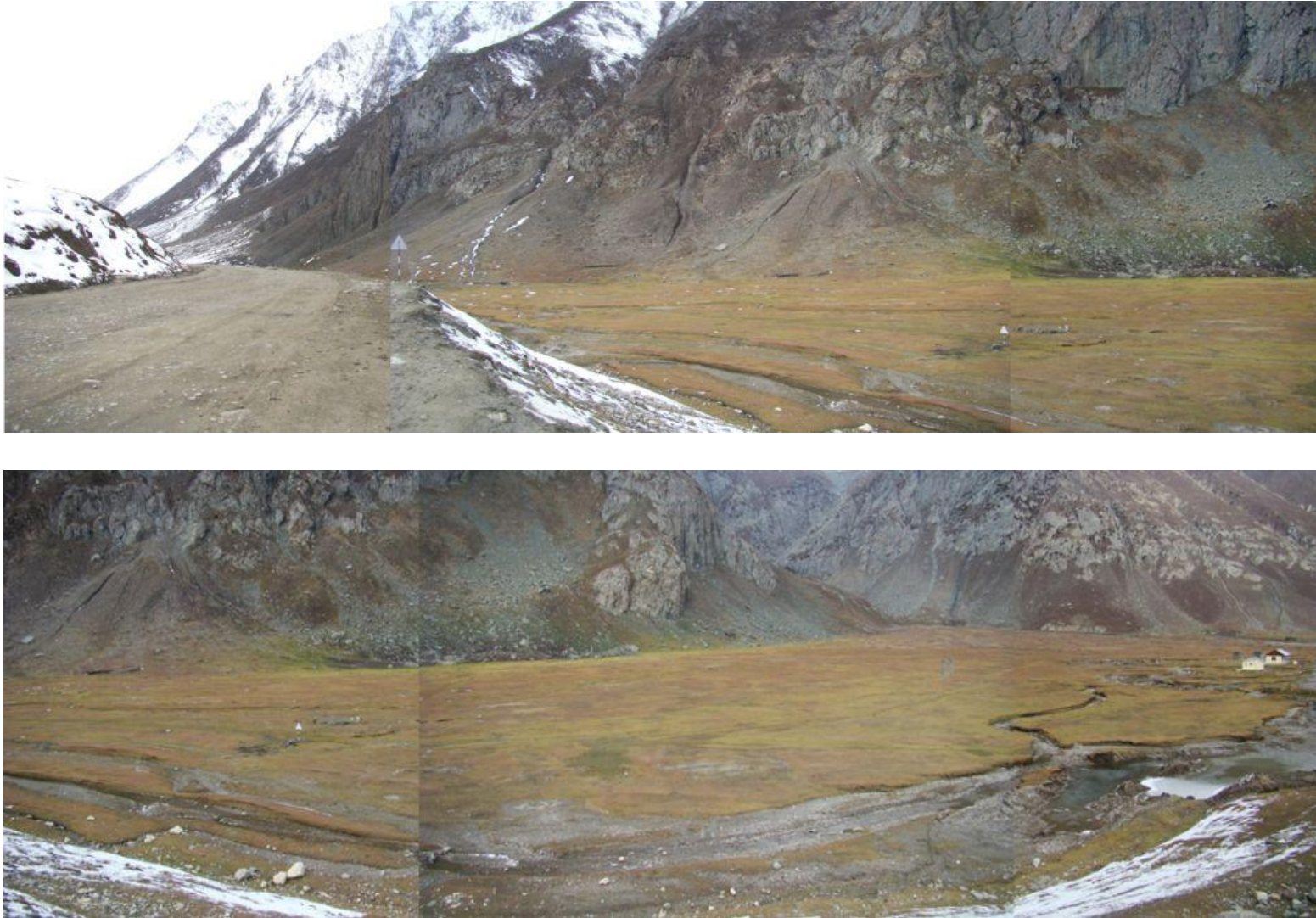


Fig. 56 Another Alignment View of Zoji-La Tunnel near Gumri Camp area



Fig. 57 Another Alignment View of Zoji-La Tunnel near Zoji – La Pass area



Fig. 58 Another Alignment View of Zoji-La Tunnel near Sytani nalla area

## 6.0 ENGINEERING GEOLOGY

Geotechnical properties of the rocks likely to be encountered at the site are being enumerated here.

### Intact Rock Properties

The summary of intact rock properties is presented in Table 2. The following geological description was found applicable for the rock chunks:

- |      |                |   |                     |
|------|----------------|---|---------------------|
| i)   | Metabasics     | : | Green in colour     |
| ii)  | Graphitic rock | : | Slightly greyish    |
| iii) | Slate          | : | Blackish in colour. |

Due to various constrains at the site 38 mm diameter cores were used for testing. The chunks were drilled to get cores of 38 mm diameter. A lapping and polishing machine was used for grinding the end-surfaces of specimens to make end-surfaces parallel to each other and perpendicular to the axis of the core. Finally, end-surfaces were made smooth with polishing machine and manual grinding on fine sand.

Unit weight was obtained by calculating the volume of the cores and measuring their weights in air-dried conditions. For specific gravity, the rock was ground to powder form and density bottle was used to determine the specific gravity as per the procedure laid in IS2720-Part III, sec-2.

Brazilian tests were conducted on discoidal specimens in dry condition as per the procedure given in ISRM (1979) and IS:10082-1981. The load was applied continuously at a constant rate so that failure of rock occurred within 15 to 30 seconds. The tensile strength is calculated using the expression,

$$\sigma_t = \frac{2P}{\pi d.t} \quad (4.1)$$

where,

- |   |   |                          |                            |     |
|---|---|--------------------------|----------------------------|-----|
| P | = | load applied at failure; | d=diameter of the specimen | and |
| t | = | thickness of specimen.   |                            |     |

Point load strength index test is an indirect test to get the uniaxial compressive strength and tensile strength of intact isotropic rock. The specimen is tested between two hardened conical tips



having 5mm curvature and 60° conical angle in rigid frame. The point load strength index ( $I_{s50}$ ) is given as:

$$I_{s50} = \frac{P}{d^2} \quad (4.2)$$

where P is the failure load and d is the size of the specimen (50 mm) measured after placing between the conical caps. The compressive strength is given by

$$\sigma_c = K I_{s50} \quad (4.3)$$

The value of K varies between 15 to 35 for most rocks; often it is taken in the range of 20-25 (Ramamurthy, 2007). In present case it is taken equal to 20. The tensile strength is given as (Ramamurthy, 2007)

$$\sigma_t = 1.25 I_{s50} \quad (4.4)$$

When 50 mm size pieces are not available, the index is calculated by making size correction as follows:

$$I_{s50} = \left( \frac{d}{50} \right)^{0.45} \left( \frac{P}{d^2} \right) \quad (4.5)$$

Uniaxial compression tests were conducted on cylindrical specimens ( $l/d \approx 2.0$ ) as suggested in ISRM (1979) suggested Methods and IS:9143-1979. Cylindrical cores of 38 mm diameter were used in the tests. Axial deformation was measured during the test. The tests were performed using a 3.0 MN conventional universal testing machine having an accuracy of  $\pm 0.1$  kN. Teflon sheets of 0.5 mm thickness were introduced at the two ends of the specimens to facilitate uniform distribution of stresses and to minimize the end-friction. In each experiment, the axial loading was gradually increased with a uniform rate such that the failure occurred in 5-10 minutes. The failure of test specimens occurred due to vertical splitting in majority of cases. The values of tangent modulus  $E_{t50}$  was computed at 50% of failure stress. The Rocks were classified as per Deere and Miller classification (1966).

Conventional axi-symmetric triaxial compression tests were conducted on rock specimens of  $l/d \approx 2.0$  as per ISRM (1981,1983) suggested methods and (IS:13047-1991). The shear strength parameters have been obtained using two failure criteria namely, Mohr-Coulomb and Hoek-Brown criterion. The Mohr-Coulomb parameters, c and  $\phi$  have been obtained by plotting p-q diagram and fitting best straight line.

Mohr failure envelope: The original Hoek-Brown (1980) criterion was used to describe the non-linear strength behaviour of intact rocks. The confined strength of the intact rock is represented as follows:

$$\sigma_1 = \sigma_3 + \sqrt{m\sigma_{ci}\sigma_3 + \sigma_{ci}^2} \quad (4.6)$$

Where  $m$  and  $\sigma_{ci}$  are the criterion parameters,

$\sigma_1$  = the major principal stress at failure,  $\sigma_3$  = the minor principal stress at failure.

The above equation was converted into linear form. The parameters were obtained by using least squares method.

**Table 2. Summary of intact rock properties**

Property	Rock type	Value
Average unit weight	Metabasic	2.81 g/cc
Average unit weight	Slate	2.43 g/cc
Specific gravity	Metabasic	2.85
Specific gravity	Graphitic rock	2.34
Specific gravity	Slate	2.49
Average tensile strength (Brazilian)	Metabasic	7.51 MPa
Average tensile strength (Brazilian)	Slate	12.23 MPa
Average UCS from point load index	Metabasic	176.56 MPa
Average UCS from point load index	Slate	85.75
Average UCS from UCS tests	Metabasic	121.55 MPa
Estimated average UCS from UCS tests	Slate	57.56 MPa
Average $E_{t50}$	Metabasic	19.0 GPa
Deere-Miller classification	Metabasic	BL
Mohr-Coulomb shear strength parameters	Metabasic	$c = 24.65 \text{ MPa}$ $\phi = 41.5^\circ$
Hoek-Brown strength parameters	Metabasic	$\sigma_{ci} = 108.15 \text{ MPa}$ $m_i = 10.29$
Hoek-Brown strength parameters ( $m_i$ from literature)	Slate	$\sigma_{ci} = 57.0 \text{ MPa}$ $m_i = 7.0$

### Rock Joint Properties

The geological observations discussed earlier present the details of the joints observed at the site. A rough idea about the joint properties can be obtained from these observations. It may however be noted that detailed mapping of joints along the tunnel alignment will be required to have higher confidence in the analysis. Nevertheless, for preliminary analysis these observations have been used. In general, there are four or more prominent joints sets encountered at various locations. A statistical analysis of dip-directions of the all the joints was carried out (Fig. 59). The analysis indicates the occurrence of the following four sets of joints plus random joints:

- i. The most dominant joint set is expected to have dip direction between the range of 35 to 75° with most likely value of 65°. The average dip is observed to be 44°.
- ii. The second joint set is likely to have its dip-direction varying from 85 to 95°, with most likely value of 95°. The average dip of the joints belonging to this family is found to be 25°.
- iii. The third set of joints is likely to have its dip-direction in the range of 125 to 145° with most likely value of 135° with an average dip of about 21°.
- iv. The fourth set of joints is likely to have dip-direction in the range of 155 to 175°, with most likely value of 165° with an average dip of 45°.
- v. Joints with random dip and dip-directions are also expected.

The rocks in the area are reported to be foliated. Figure 60 shows the statistical analysis of the dip-directions of the foliation planes. There are four families of dip-directions of the foliation planes as given below:

- i. Ranging between 155 to 185°,
- ii. Having dip-direction of 235°
- iii. Ranging between 285 to 305°,
- iv. Ranging from 335 to 345°.

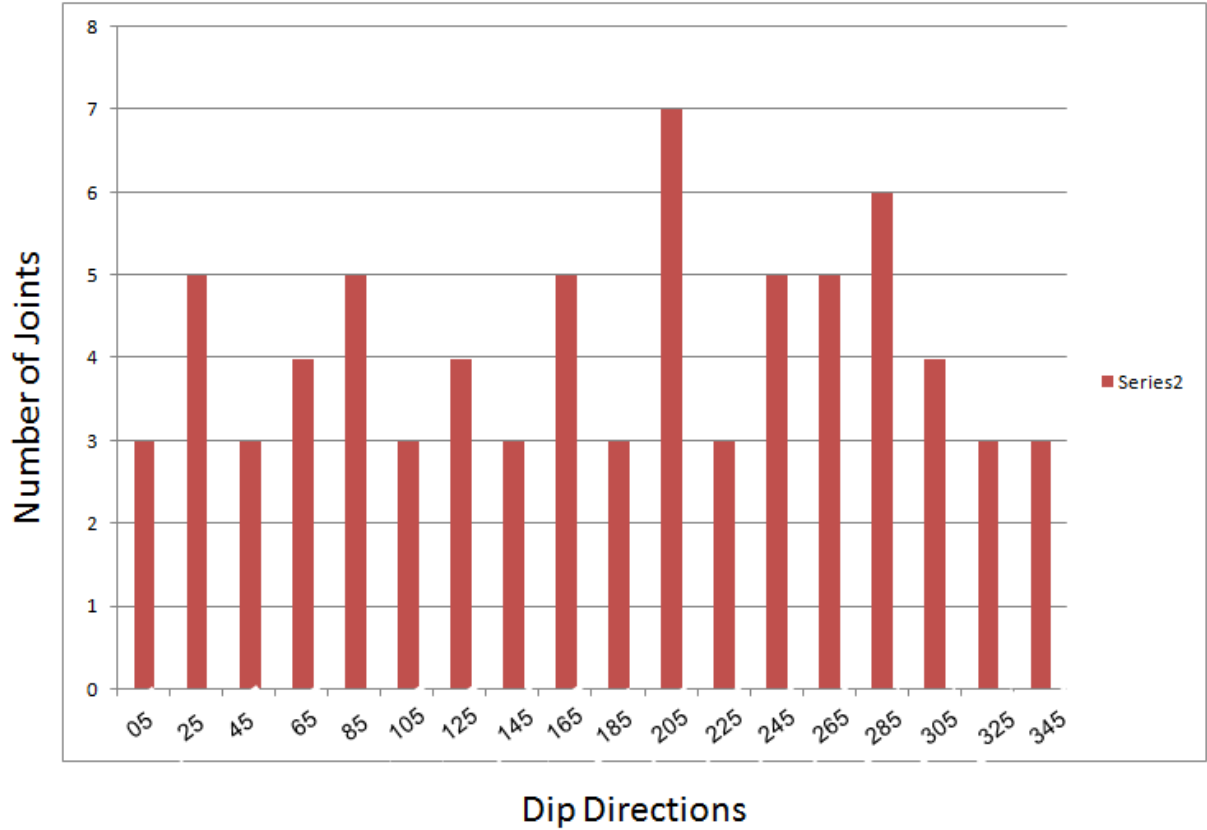


Fig. 59a Statistical analysis of dip-directions of joints (Zoji-La Tunnel Project)

The assessment of the mechanical properties of the rock joints needs much more data from the exact location of the structures. The observations made on surface generally describe joints to be open. In the opinion of the authors, the joints will not remain open when acting under large overburden. It is therefore expected that the closed joints will be intersected in the tunnel except close to the portals or if the overburden is low. At the site simple tests like tilt tests can be performed to get the frictional characteristics of the joint surfaces. In absence of such information Barton's model can be used to roughly estimate the shear strength parameters of rock joints. As per this model the shear strength along the joint is expressed as:

$$\tau_f = \sigma_n \tan \left[ \phi_r + JRC \log_{10} \frac{JCS}{\sigma_n} \right] \quad (4.7)$$

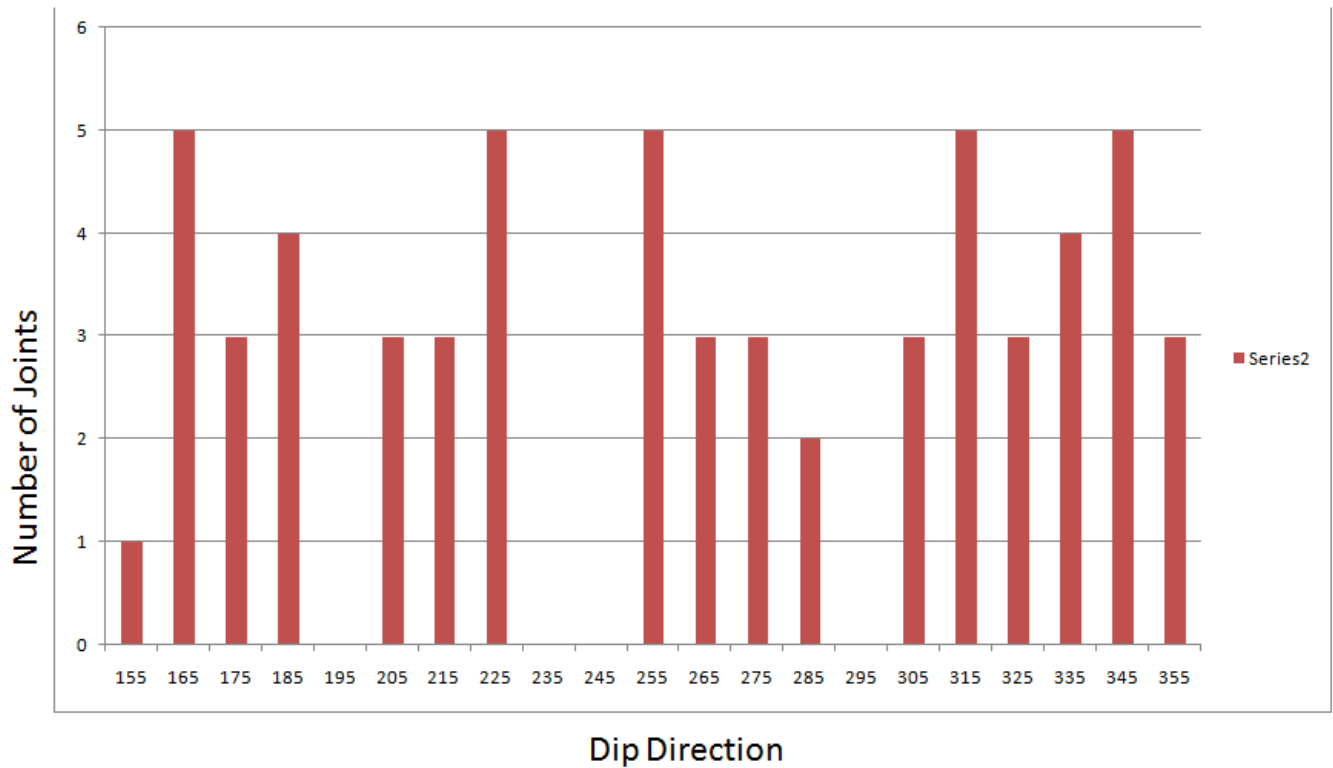


Fig. 59b Statistical analysis of dip-directions of foliation planes

(Zoji-La Tunnel Project)

Where  $\phi_r$  is residual friction angle, JRC is the joint roughness coefficient, which is a measure of the initial roughness (in degrees) of the discontinuity surface. JRC is assigned a value in the range of 0–20, by matching the field joint surface profile with the standard surface profiles on a laboratory scale of 10 cm (Barton and Choubey, 1977). JCS is the joint wall compressive strength of the discontinuity surface, and  $\sigma_n$  is the effective normal stress acting across the discontinuity surface.

In geological observations the discontinuities have been reported to be rough in majority cases. In very few cases smooth roughness is also reported. Simulated values of shear strength were plotted against normal stress; results are presented in Figs. 4.2. An approximate estimate of shear strength parameters is as follows:

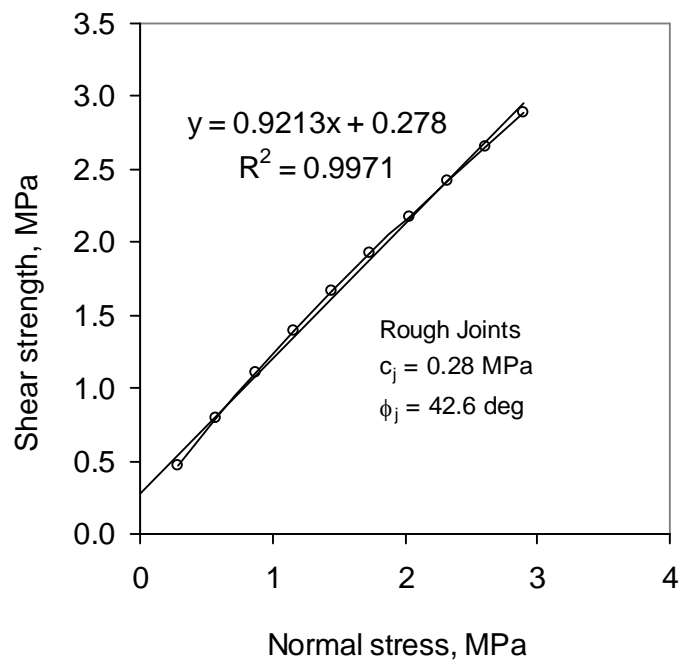


Fig 60a Simulated shear strength envelope from Barton's model  
(Rough joints: JRC= 12)

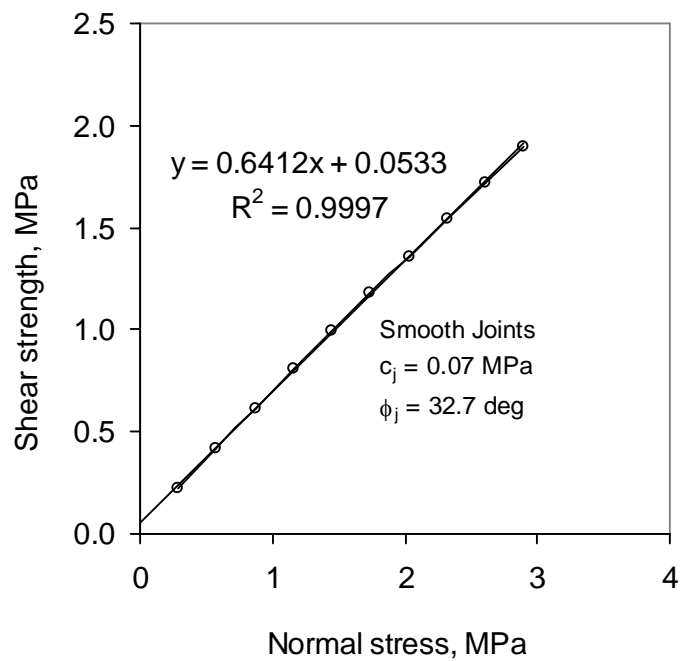


Fig 60b. Simulated shear strength envelope from Barton's model  
(Smooth joints: JRC= 4)

- i. Rough joints;  $c_j = 0.28\text{MPa}$ ,  $\phi_j = 42.6$  degrees.
- ii. Smooth joints  $c_j = 0.07\text{ MPa}$ ,  $\phi_j = 32.7$  degrees.

### Rock Mass Modulus

The best estimate of rock mass deformability can only be made from the results of the field tests. This data will be available only after the detailed investigation. In the absence of such data, deformability characteristics may be estimated approximately from classification approaches and laboratory test data.

Hoek and Diederichs (2006) have suggested the following expressions for the rock mass modulus based on GSI:

$$E_{\text{mass}} = E_i \left( 0.02 + \frac{1 - D/2}{1 + \exp((60 + 15D - \text{GSI})/11)} \right) \quad (4.8)$$

$$E_{\text{mass}} = 1 \times 10^5 \left( \frac{1 - D/2}{1 + \exp((75 + 25D - \text{GSI})/11)} \right) \quad (4.9)$$

where  $E_i$  is the intact rock modulus and  $D$  is the damage factor.

Barton (2002) has suggested the following expression for rock mass modulus in terms of rock mass quality,  $Q$ :

$$E_{\text{mass}} = 10Q_c^{1/3} \text{ GPa} \quad (4.10)$$

$$\text{where } Q_c = Q \frac{\sigma_{ci}}{100} \quad (4.11)$$

$\sigma_{ci}$  is the intact rock strength in MPa.

The Rock Mass Rating (RMR) may be used to estimate rock mass modulus as follows:

- Serafim and Pereira (1983)



$$E_{\text{mass}} = 10^{(\text{RMR}-10)/40} \text{ GPa} \quad (4.12)$$

- Mehrotra (1992):

$$E_{\text{mass}} = 10^{(\text{RMR}-25)/40} \text{ GPa} \quad (4.13)$$

- Ramamurthy (2007)

$$E_{\text{mass}} = E_i \exp\left(\frac{\text{RMR} - 100}{17.4}\right) \quad (4.14)$$

Geotechnical investigations are required to be done with an aim of characterising the rock mass available at different section along the tunnel alignment. It is suggested that various classification systems (RQD, Q, RMR and GSI) should be used independently to characterise the rock mass. The rock mass then should be divided into several classes and should be analysed for tunnel support pressure etc. In absence of any such detailed investigation a rough exercise was done by using the photographs of various locations. GSI was assigned and RMR and Q were estimated from assigned GSI. The following expressions were used to estimate Q and RMR.

$$\text{GSI} = \text{RMR} - 5 \quad (4.15)$$

$$\text{RMR} = 9 \ln Q + 44 \quad (4.16)$$

It should be noted that this analysis is very preliminary and its results should be used to get the idea about the characterisation of the rock mass.

The rock mass modulus values obtained from the above expressions (using slate properties) are presented in Table 3. The average values of the estimated rock mass modulus are also presented in the table.

Table 3. Estimated rock mass modulus from different approaches

Sl	GSI	RMR	Q	Rock mass modulus (GPa)						
				Hoek and Diederichs (2006)-1	Hoek and Diederichs (2006)-2	Barton (2002)	Ramamurthy (2007)	Mehrotra (1992)	Serafim and Pereira (1983)	Average
1	17	22	0.085	0.745	0.513	3.685	0.218	0.839	1.987	1.153
2	22	27	0.155	0.969	0.802	4.443	0.286	1.122	2.661	1.713
3	25	30	0.207	1.139	1.057	4.971	0.343	1.337	3.161	1.989
4	30	35	0.373	1.555	1.645	5.976	0.453	1.772	4.220	2.611
5	35	40	0.645	2.155	2.567	7.191	0.612	2.365	5.623	3.419
6	40	45	1.123	3.038	3.986	8.655	0.825	3.161	7.492	4.524
7	45	50	1.948	4.252	6.138	10.412	1.073	4.231	10.023	6.011
8	50	55	3.388	5.836	9.341	12.535	1.431	5.621	13.345	8.012
9	55	60	5.915	7.753	13.965	15.084	1.907	7.456	17.745	10.666

### Uniaxial Compressive Strength of Rock Mass

Rock mass strength under uniaxial loading condition has been estimated by the following approaches:

- i) Yudhbir & Prinzl (1983)

$$\frac{\sigma_{cm}}{\sigma_{ci}} = \exp\left(\frac{7.65 \times (RMR - 100)}{100}\right) \quad (4.17)$$

- ii) Laubscher (1984) and Singh and Goel (1999)

$$\frac{\sigma_{cm}}{\sigma_{ci}} = \frac{RMR - \text{Rating for } \sigma_{ci}}{106} \quad (4.18)$$

- iii) Ramamurthy et al. (1985) and Ramamurthy (1986)

$$\frac{\sigma_{cm}}{\sigma_{ci}} = \exp\left(\frac{RMR - 100}{18.75}\right) \quad (4.19)$$

iv) Trueman (1988) and Asef et al. (2000)

$$\sigma_{cm} = 0.5 \exp(0.06 RMR) \text{ MPa} \quad (4.20)$$

v) Kalamaras and Bieniawski (1993)

$$\frac{\sigma_{cm}}{\sigma_{ci}} = \exp\left(\frac{RMR - 100}{24}\right) \quad (4.21)$$

vi) Sheorey (1997)

$$\frac{\sigma_{cm}}{\sigma_{ci}} = \exp\left(\frac{RMR - 100}{20}\right) \quad (4.22)$$

vii) Aydan and Dalgic, (1998)

$$\frac{\sigma_{cm}}{\sigma_{ci}} = \frac{RMR}{RMR + 6(100 - RMR)} \quad (4.23)$$

viii) Singh and Rao (2005)

$$\frac{\sigma_{cm}}{\sigma_{ci}} = \left(\frac{E_{mass}}{E_i}\right)^{0.63} \quad (4.24)$$

where  $\sigma_{cm}$  = rock mass strength

$E_{mass}$  = rock mass modulus

$E_i$  = intact rock modulus.

ix) Singh et al. (1997)

$$\sigma_{cm} = 7\gamma Q^{1/3} \quad (\text{for } Q < 10, 2 < \sigma_{ci} < 100 \text{ MPa, SRF} = 2.5) \quad (4.25)$$

where  $\gamma$  is unit weight in gm/cc.

x) Barton (2002)

$$\sigma_{cm} = 5\gamma \left(\frac{Q\sigma_{ci}}{100}\right)^{1/3} \quad (4.26)$$

The above mentioned approaches were used to estimate the rock mass strength values. The results are presented in Table 4 where average values are also reported. It can be noted that depending on characterisation of a particular location the average value of rock mass strength may be taken in the range of about 5 to 22 MPa.

### Triaxial Strength of Rock Mass

Mohr-Coulomb shear strength parameters of the rock mass ( $c_{\text{mass}}$  and  $\phi_{\text{mass}}$ ) are required to compute the triaxial strength of the rock mass. A procedure suggested by Hoek and Brown (1997) has been adopted for this purpose. As per this approach, the strength of the rock mass is represented by the generalised criterion as:

$$\sigma_1 = \sigma_3 + \sigma_{ci} \left( \frac{m_j \sigma_3}{\sigma_{ci}} + s_j \right)^a \quad (4.27)$$

The parameters,  $m_j$ ,  $s_j$  and 'a' are estimated from the following relationships:

$$m_j = m_i e^{\left( \frac{GSI-100}{28} \right)} \quad (4.28)$$

- i) For undisturbed rock masses i.e GSI > 25

$$s_j = e^{\left( \frac{GSI-100}{9} \right)} \quad (4.29)$$

$$a = 0.5$$

**Table 4. Estimated rock mass strength**

Sl	GSI	RMR	Q	Rock mass strength (MPa)														
				Yudhbir & Prinzl, MPa	Laubscher (1984)	Ramamurthy (1993)	Trueman (1988)	Kalamaras & Bieni awski (1993)	Sheorey (1997)	Aydan & Dalgic (1998)	E _{mass} from Deiderich -1	E _{mass} from Hoek, Deiderich -2	E _{mass} from Barton	E _{mass} from Ramamurthy (RMR)	E _{mass} from Mehrotra (1992)	Barton (2002)	Singh et al, (1997)	Average
1	17	22	0.085	0.14	5.44	0.89	1.85	2.20	1.21	2.55	7.52	5.91	20.35	3.45	8.3	4.55	7.59	5.81
2	22	27	0.154	0.23	8.23	1.23	2.51	2.74	1.54	3.33	8.86	7.85	23.22	4.10	9.73	5.59	9.32	6.34
3	25	30	0.209	0.25	9.82	1.34	3.02	3.21	1.73	3.78	9.85	9.31	24.82	4.50	10.1	6.23	10.22	7.51
4	30	35	0.363	0.41	12.6	1.84	4.08	3.81	2.22	4.71	12.2	12.40	27.49	5.55	13.3	7.47	12.74	8.67
5	35	40	0.640	0.58	15.4	2.31	5.51	4.65	2.86	5.67	14.9	16.41	31.45	6.59	15.5	8.85	15.30	10.14
6	40	45	1.112	0.85	17.9	3.20	7.44	5.77	3.70	6.91	18.1	21.64	35.34	7.92	18.1	10.6	18.12	12.74
7	45	50	1.943	1.31	20.8	3.93	9.98	7.29	4.76	8.35	22.2	28.40	39.62	9.42	22.8	13.4	21.84	15.28
8	50	55	3.389	1.83	23.4	5.19	13.7	8.75	6.14	9.85	27.6	37.12	44.63	11.34	26.7	15.6	26.33	18.45
9	55	60	5.915	2.71	26.3	6.86	18.4	10.85	7.82	11.5	32.8	47.75	50.11	13.61	32.3	18.8	31.60	22.21

ii) For disturbed rock masses,  $GSI < 25$

$$s = 0$$

$$a = 0.65 - \frac{GSI}{200} \quad (4.28)$$

where, GSI is the geological strength index.

By following the above expressions, parameters  $m_j$ ,  $s_j$  and 'a' were obtained for two extreme GSI values i.e. 17 and 55 respectively. Now the values of simulated tri-axial strength were generated for eight confining stresses in the range of  $0 < \sigma_3 < 0.25 \sigma_{ci}$  as suggested by Hoek and Brown (1997). The equivalent Mohr-Coulomb shear strength parameters,  $c_{mass}$  and  $\phi_{mass}$  were now obtained by fitting a straight line into the simulated tri-axial tests data and using the following expressions:

$$\phi_{mass} = \sin^{-1} \left( \frac{k-1}{k+1} \right) \quad (4.29)$$

$$c_{mass} = \frac{\sigma_{cm}}{2\sqrt{k}} \quad (4.30)$$

where the best fitting straight line is given as:

$$\sigma_1 = \sigma_{cm} + k\sigma_3 \quad (4.31)$$

The results are presented in Figs. 61. The representative values of the shear strength parameters of the rock mass are presented in Table 5.

Table 5. Hoek- Brown and equivalent Mohr-Coulomb shear strength parameters

GSI	$m_i$	$\sigma_{ci}$ , MPa	$m_j$	$s_j$	a	$c_{mass}$ MPa	$\phi_{mass}$ (degrees)
17	7	58.0	0.3722	0.0	0.561	0.45	24.20
55	7	58.0	1.4135	0.0065	0.47	1.86	34.70



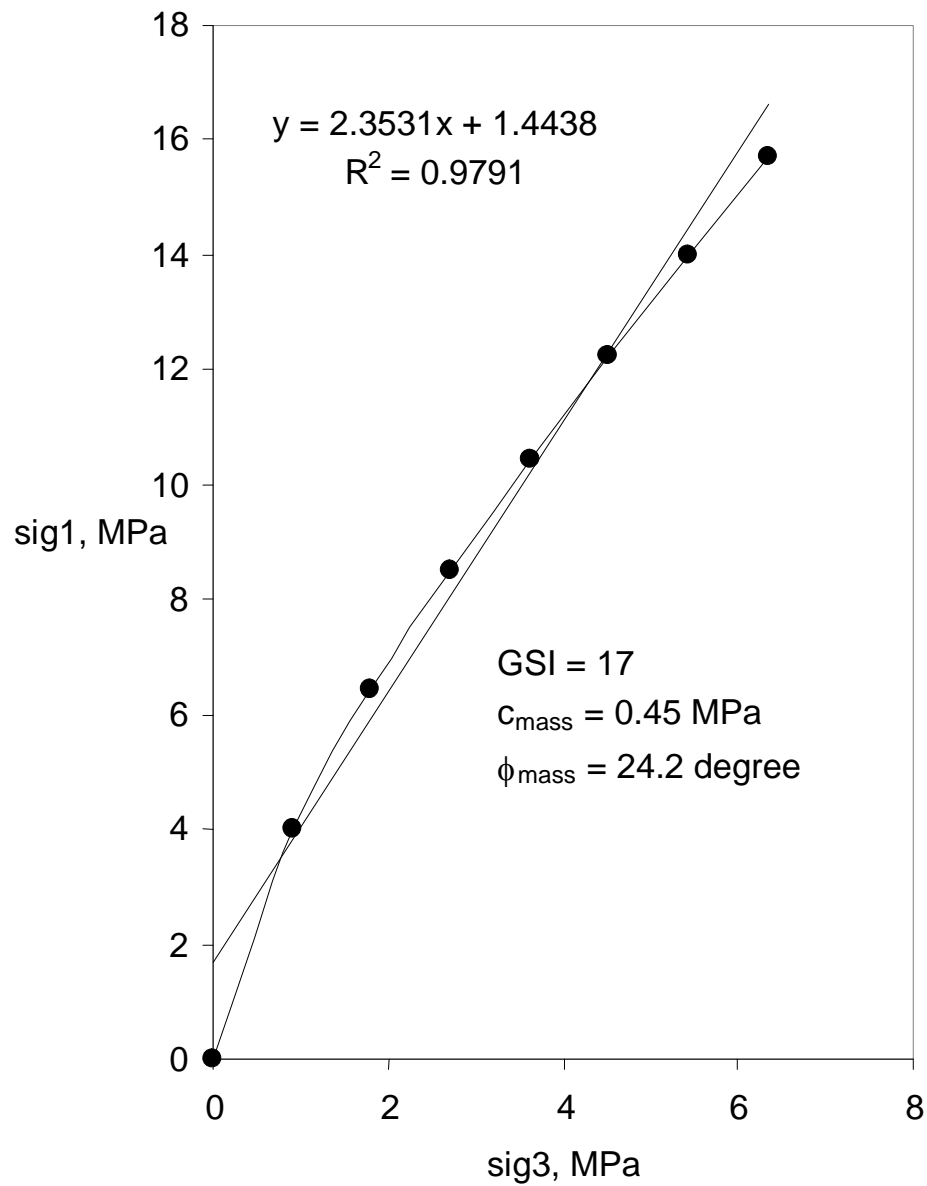


Fig. 61 a Shear strength parameters of rock mass through Hoek-Brown failure (GSI = 17)

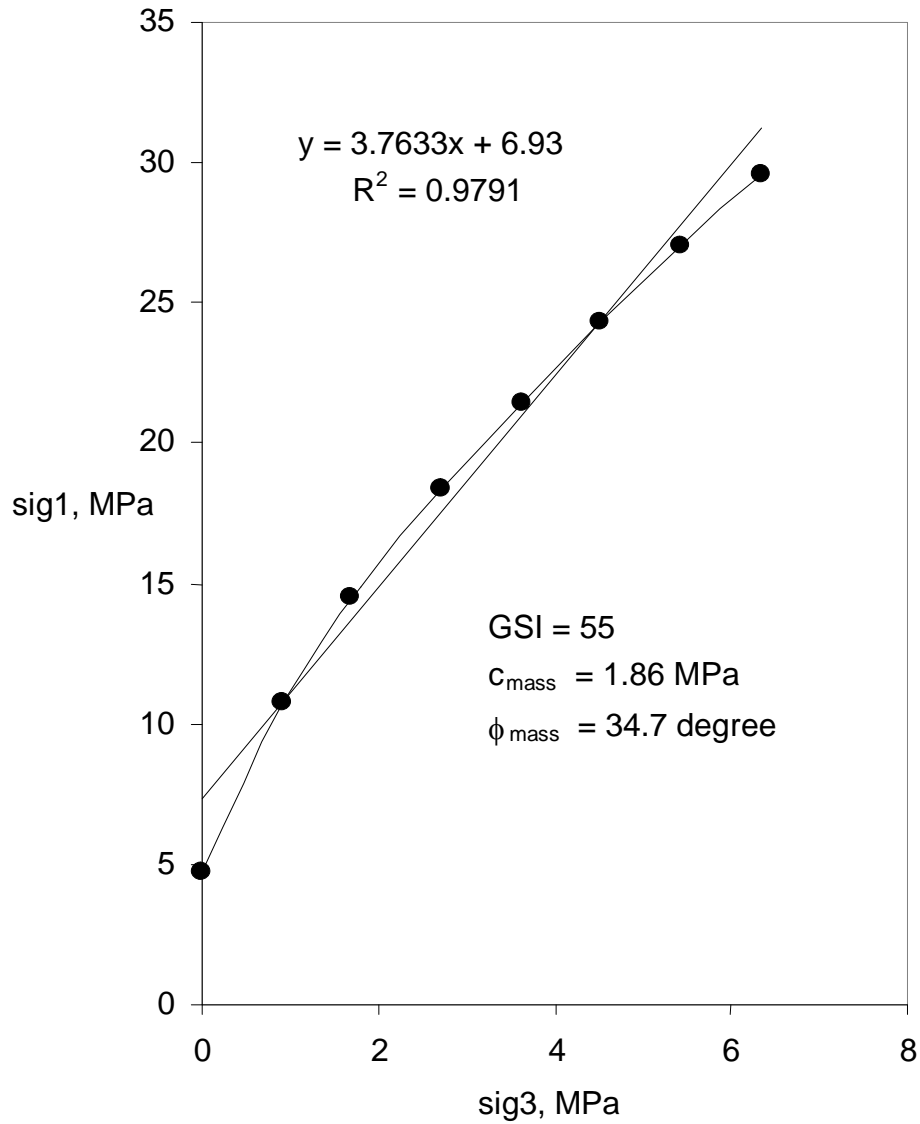


Fig. 61 b Shear strength parameters of rock mass through Hoek-Brown failure (GSI = 55)

## Squeezing and rock burst

A maximum rock cover of about 970m is expected above the tunnel roof. An estimate of squeezing potential may be obtained from the ratio of circumferential stress to the strength of the rock mass at the periphery of the tunnel as given in Table 6. In the present case rock mass strength has been found to vary between 5 to 22 MPa depending on the rock mass characterization. Taking maximum circumferential stress equal to  $2 \gamma H$ , the  $\sigma_\theta$  works out to be 48.6 MPa. The ratio  $\sigma_\theta / \sigma_{cm}$  may vary from 9.72 to 2.20. This indicates that conditions from moderate to high squeezing may be expected during tunnel construction. The intermediate principal stress may however play important role and squeezing may reduce because of strength enhancement due to intermediate principal stress.

**Table 6. Suggested predictions of squeezing conditions**

Degree of squeezing	$\sigma_\theta / \sigma_{cm}$ (ISRM)	$\sigma_{cm} / (\gamma H)$ (Barla)
Non squeezing	< 1.0	>1.0
Mild squeezing	1.0 – 2.0	0.4 – 1.0
Moderate squeezing	2.0 – 4.0	0.2 – 0.4
High squeezing	> 4.0	<0.2

**BIBLIOGRAPHY**

- Auden, J.B., 1935, Traverses in the Himalayas, Rec. Geol. Surv. Ind., 69 (2) Bologne.
- Asef M. R., Reddish D. J., Lloyd P. W. (2000) Rock-support interaction analysis based on numerical modeling, *Geotech. Geol. Eng.*, 18:23–37.
- Aydan O., Dalgic S. (1998) Prediction of deformation behavior of 3-lanes Bolu tunnels through squeezing rocks of North Anatolian fault zone (NAFZ). In: *Proceedings of regional symposium on sedimentary rock engineering*, Taipei, pp 228–233.
- Barla, G., 2001. Tunnelling under squeezing rock conditions. Tunnelling mechanics. In: *Kolymbas* (Ed.), Eurosummer-School in Tunnel Mechanics, Innsbruck, 2001, Logos Verlag, Berlin, pp. 169–268. Available at: [http://ulisse.polito.it/matdid/1ing_civ_D3342_TO_0/Innsbruck2001.PDF](http://ulisse.polito.it/matdid/1ing_civ_D3342_TO_0/Innsbruck2001.PDF)>.
- Barton N. (2002) Some new Q-value correlations to assist in site characterisation and tunnel design, *Int. J. Rock Mech. & Min. Sci.*, 39: 185–216.
- Barton, N. and Chobey, V. (1977), “The Shear Strength of Rock Joints in Theory and Practice”, *Rock Mechanics*, 10, 1-54.
- Desio, A., Tongiorgi, E. and Ferrara, G., 1964, on the geological age of some granites of Karakoram, Hindukush and Badakhshan (Central Asia), *Proc, 22nd . Inter. Geol. Cong.*, 2, 479-496.
- Hoek E. and Bray J.W. (1981) *Rock Slope Engineering*, Revised 3rd edition, The Institution of Mining and Metallurgy, London, pp 341 – 351.
- Hoek E., Brown E.T. (1997) Practical estimates of rock mass strength. *Int. J. Rock Mech. Min. Sci.*, 34:1165–1186.
- Hoek E., Diederichs M. S. (2006) Empirical estimation of rock mass modulus. *Int. J. Rock Mech. Min. Sci.*, 36:203–215.
- Kalamaras G. S., Bieniawski Z. T. (1993) A rock mass strength concept for coal seams. In: *Proceedings of 12th conference ground control in mining*, Morgantown, pp 274–283.

Laubscher D. H., (1984) Design aspects and effectiveness of support system in different mining conditions. *Trans. Inst. Min. Met.*, 93:A70–A81.

Mathur, Y. K. and Jain, A. K., 1973, palynology and age of the Dras Volcanics near Shergol,

Mehrotra V. K. (1992) *Estimation of Engineering Parameters of Rock Mass*, Ph.D. thesis, University of Roorkee, Roorkee, India.

Ramamurthy T., Rao G.V., Rao K. S. (1985) A strength criterion for rocks. In: *Proceedings of Indian geotechnical conference*, Vol 1, Roorkee, pp 59–64.

S.K Shah, Madan L. Sharma, J. T. Gergan and C.S. Tara (1976), *Stratigraphy & Structure of the Western part of the Indus Suture Belt, Ladakh, Northwest Himalaya.*, Deptt. Of Geology, University of Jammu, Jammu.

Serafim J. L., Pereira J. P. (1983) Consideration of the geomechanical classification of Bieniawski. In: *Proceedings of international symposium on engineering geology and underground construction*, Lisbon, Portugal, Vol 1(II), pp 33–44.

Sheorey P. R. (1997) *Empirical rock failure criteria*. Balkema, Rotterdam.

Singh B, Viladkar MN, Samadhiya NK, Mehrotra VK. (1997) Rock mass strength parameters mobilised in tunnels. *Tunnelling and Underground Space Technology*, 12(1), 47 - 54.

Singh M., Rao K. S. (2005) Empirical methods to estimate the strength of jointed rock masses. *Eng. Geol.*, 77(1–2):127–137.

Trueman R. (1988) An evaluation of strata support techniques in dual life gateroads. Ph.D. thesis, University of Wales, Cardiff.

Yudhbir W. L., Prinzl F. (1983) An empirical failure criterion for rock masses. In: *Proceedings of 5th international congress on Rock Mechanics*, Vol. 1, Melbourne, pp B1–B8.

Wadia ,D.N., 1937, The cretaceous and Volcanic series of Astor, Deosai Kashmir and its Intrusions, *Rec. Geol. Surv. India*. 72 (2), 151-61.